Imaging, Diagnosis, Prognosis

Clinical Cancer Research

Secreted Protein Acidic and Rich in Cysteines-like 1 Suppresses Aggressiveness and Predicts Better Survival in Colorectal Cancers

Hanguang Hu[1], Hang Zhang[1], Weiting Ge[1], Xiyong Liu[2], Sofia Loera[3], Peiguo Chu[3], Huarong Chen[1], Jiaping Peng[1], Lun Zhou[1], Shujing Yu[1], Ying Yuan[1], Suzhan Zhang[1], Lily Lai[4], Yun Yen[2], and Shu Zheng[1]

Abstract

Purpose: *Secreted protein acidic and rich in cysteines-like 1* (*SPARCL1*) is an extracellular matrix glycoprotein with malignancy-suppressing potential. The hypothesis that *SPARCL1* reduces cancer invasiveness and predicts better survival in colorectal cancers (CRC) was investigated.

Experimental Design: Stable *SPARCL1* transfectants, RKO-*SPARCL1*, and corresponding vector control were constructed and implanted into nude mice to generate a mouse xenograft model of liver metastasis. Also, a retrospective outcome study was conducted on the COH set (222 CRCs) and ZJU set (412 CRCs). The protein expression level of *SPARCL1* was determined by immunohistochemistry. The Kaplan–Meier and Cox analyses were used for survival analysis. The association of *SPARCL1* with mesenchymal–epithelial transition (MET) was examined by reverse transcription PCR (RT-PCR) and Western blot analysis.

Results: The ectopic expression of *SPARCL1* significantly reduced the potential for anchorage-independent growth, migration, invasion and induced cell differentiation in RKO and SW620 cells. In mouse xenograft model, the expression of *SPARCL1* significantly reduced the liver metastasis ($P < 0.01$). The patient-based studies revealed that the expression of *SPARCL1* was related to better differentiation ($P < 0.01$), less lymph node involvement [OR, 0.67; 95% confidence interval (CI), 0.45–1.00], and less distant metastasis (OR, 0.38; 95% CI, 0.18–0.79). The Kaplan–Meier and Cox analysis showed that the expression of *SPARCL1* was associated with better overall survival (log-rank: $P < 0.01$; HR, 0.57; 95% CI, 0.39–0.84). Transfection of *SPARCL1* induced MET of colon cancer cells.

Conclusion: *SPARCL1* functions as a tumor suppressor promoting differentiation possibly via MET, which inhibits the aggressiveness of CRCs. *Clin Cancer Res; 18(19); 5438–48. ©2012 AACR.*

Introduction

Colorectal cancer (CRC) is one of the leading causes of cancer mortality in the world (1). Despite improvements in early detection and treatment of CRC in the last few decades, the 5-year survival rate remains about 50% to 60% (2, 3). This high mortality is partially attributable to liver metastasis which accounts for 40% to 50% of recurrences in patients with CRCs (4). Exploring the molecular basis of liver metastasis may provide further improvements in early detection, prevention, intervention, and prognostic evaluation for patients with CRCs.

Secreted protein acidic and rich in cysteines (*SPARC*) family includes *SPARC*, *SPARCL1*, and *SMOC-2*. *SPARCL1*, which is also known as *Hevin*, *SC1*, or *MAST9*, is an extracellular matrix (ECM) glycoprotein, whose gene is located in 4q22 (5, 6). *SPARCL1* was first isolated from a human high endothelial venules cDNA library and is involved in many physiologic functions, such as cell adhesion (7, 8), cell proliferation (7), central nervous system development (9), and B-lymphocyte maturation (10). *SPARCL1* is widely expressed in normal tissues such as brain, heart, lung, muscle, colon, and kidney (5, 6, 11–13). In contrast, its full-length expression was strongly downregulated in several carcinomas such as metastatic prostate adenocarcinoma and non–small cell lung cancer (5, 8, 14–16). The downregulation of *SPARCL1* mRNA in colorectal carcinomas was confirmed by Northern blotting (9) and oligonucleotide array (17). Previously, pilot studies showed that

Authors' Affiliations: [1]Cancer Institute (Key Laboratory of Cancer Prevention and Intervention, China National Ministry of Education), The Second Affiliated Hospital, School of Medicine, Zhejiang University, Hangzhou, Zhejiang, China; and Departments of [2]Molecular Pharmacology, [3]Anatomic Pathology, and [4] Surgical Oncology, City of Hope National Medical Center, Duarte, California

Note: Supplementary data for this article are available at Clinical Cancer Research Online (http://clincancerres.aacrjournals.org/).

H. Hu and H. Zhang are co-first authors.

Corresponding Authors: Shu Zheng, Cancer Institute, The Second Affiliated Hospital, School of Medicine, Zhejiang University, Hangzhou, Zhejiang, China, 310009. Phone: 86-571-8778-4501; Fax: 86-571-8721-4404; E-mail: zhengshu@zju.edu.cn; and Yun Yen, Department of Molecular Pharmacology, Beckman Research Institute of the City of Hope, 1500 E. Duarte Road, Duarte, CA 91010. Phone: 626-256-4673, ext. 65707; Fax: 626-471-3607; E-mail: yyen@coh.org

doi: 10.1158/1078-0432.CCR-12-0124

©2012 American Association for Cancer Research.

Downloaded from http://aacrjournals.org/clincancerres/article-pdf/18/19/5438/2005391/5438.pdf by guest on 23 May 2025

Translational Relevance

Secreted protein acidic and rich in cysteines-like 1 (SPARCL1) is an extracellular matrix glycoprotein with malignancy-suppressing potential that is vital to the development of neural system. Here, our findings displayed that *SPARCL1* inhibits cell proliferation, anchorage-independent growth, and invasion and induces differentiation in colon cancer cells. This study also explored the metastasis-suppressing ability of *SPARCL1* in a mouse xenograft model. Meanwhile, the invasion-suppressing potential of *SPARCL1* was assessed with outcome study based on two sets of patients with colorectal cancer (CRC). The findings consistently validated that high expression of *SPARCL1* was negatively associated with poor differentiation and metastasis, resulting in a better survival of CRCs. Furthermore, we showed that the *SPARCL1* induced differentiation by mesenchymal–epithelial transition in colon cancer cells. These findings provided evidences for *SPARCL1* as a potential prognostic biomarker, indicative of tumor invasion and metastasis of CRCs.

high *SPARCL1* expression level is associated with well-differentiated status, less metastasis, and better survival in CRCs (18). Similar results were obtained by other investigators that indicated that the expression of *SPARCL1* increased with greater level of differentiation and decreased in progressing from Dukes stage B to D. However, their data showed that expression of *SPARCL1* led to poor survival in CRCs (19). Therefore, the prognostic value of *SPARCL1* needs to be further investigated at multiple centers with larger population. Meanwhile, it was necessary to further explore the malignancy-suppressing ability of *SPARCL1* to clarify the mechanism(s).

In this study, we investigated whether the expression of *SPARCL1* in colon cell lines reduces cell proliferation, invasion, or metastasis in an *in vitro* setting and in a mouse xenograft model. In addition, we explored the biologic role of *SPARCL1* protein in anchorage-independent growth, migration, and differentiation of cells. Furthermore, we conducted outcome studies on 2 CRC patient sets (COH set, 222 cases; and ZJU set, 412 cases) with different racial and socioeconomic backgrounds. Two outcome studies yielded consistent findings indicating that the expression of *SPARCL1* predicts better survival in CRCs, implying that *SPARCL1* may serve as a potential prognostic biomarker for CRCs.

Materials and Methods

Cell culture and *SPARCL1* expression plasmid transfection

Colon cancer cell lines (RKO and SW620) were obtained from American Type Culture Collection. RKO was cultured in RPMI-1640 medium and SW620 cells in Leibovitz L-15 medium at 37°C in 5% CO_2. Culture medium was supplemented with 10% FBS (Gibco), penicillin (100 U/mL), and streptomycin (100 μg/mL). The human *SPARCL1* cDNA was cloned into the pLXSN retroviral expression vector (Clontech) and then transfected into the retroviral PT67 packaging cell line (Clontech) using Lipofectamine 2000 reagent (Invitrogen). After 72-hour incubation, virus-containing supernatants from PT67 cells were collected and then filtrated by 0.45-μm filters. The filtered supernatant was added to 70% confluent cells in the presence of 8 μg/mL polybrene (Sigma). After 24 hours, cells were incubated with 500 μg/mL of G418 for stable *SPARCL1* expression transfectant selection. Meanwhile, the pLXSN vector was also transfected in the same way as a control.

Antibodies

Mouse monoclonal antibodies against *SPARCL1* were produced by HuaAn Bio-Technology Co., Ltd. using synthesized peptide (aa351–364: CDGPRHSASDDYFIP) as the antigen. The efficiency of antibodies was visualized by using recombinant human *SPARCL1* protein (R&D) in Western blot analysis. The mouse monoclonal antibody IgG named No.C11 was preselected for further Western blot and immunohistochemical (IHC) staining experiments. In Western blot analysis, No.C11 significantly reduced nonspecific signals in comparison with commercial antibody (Supplementary Fig. S1). Moreover, the signal of recombinant *SPARCL1* protein and endogenous *SPARCL1* (75 KDa and 130 KDa) could be specifically blocked by recombinant *SPARCL1* full-length peptide (Supplementary Fig. S1), which indicated the specificity of antibody. The *E-cadherin* (#3195), *N-cadherin* (#4061), and *Vimentin* (#3390) antibodies were from Cell Signaling Technology and diluted as recommended. Anti-β-actin antibody was from Sigma and secondary antibodies were from Bio-Rad.

Quantitative reverse transcription PCR analysis and Western blot analysis

RNA and protein were extracted from subconfluent cells in the exponential phase of growth. Total RNA was extracted and purified using Rneasy kit (Qiagen). Each mRNA sample (4 μg) was reverse transcribed using the LongRange 25tep RT-PCR Kit (Qiagen). An ABI One-Step Real-Time PCR System (Applied Biosystem) was used for quantitative reverse transcription PCR (qRT-PCR) analysis. The experiments were carried out in triplicate and normalized by β-actin (loading control). Primer sequences applied in qRT-PCR experiments are listed in Supplementary Table S1.

Secreted protein in cell culture supernatant was extracted using Trichloroacetic Acid-Acetone (Sigma) Precipitation. Protein in 20 mL serum-free supernatant was resuspended in 20 μL loading buffer. Cell lysate samples were extracted by M-PER Mammalian Protein Extraction Reagent (Pierce) containing the protease inhibitor cocktail (Sigma). For Western blot analysis, about 40 μg lysate samples or 20 μL secreted protein were loaded into each well and separated by SDS-PAGE then transferred to polyvinylidene fluoride

Downloaded from http://aacrjournals.org/clincancerres/article-pdf/18/19/5438/2005391/5438.pdf by guest on 23 May 2025

membrane. Immunoblotting was conducted by incubation with anti-*SPARCL1* (No.C11, 1:200), *E-cadherin*, *N-cadherin*, *Vimentin*, and β-actin antibodies as mentioned above and then followed by incubation with corresponding alkaline phosphatase–conjugated second antibodies. Immunoreactive bands were visualized by enhanced-ECL or SuperSignal (Pierce).

In vitro cell growth assays

The measurement of cell proliferation was based on cell counting on 24-well plates. At initiation of the study, approximately 1×10^4 cells were seeded per well. At each time point, cells on 24-well plates were trypsinized and then harvested. For cell counting, trypan blue staining was used to indicate viable cells. The proliferative activity was also determined by MTS assay (CellTiter 96 Non-Radioactive Cell Proliferation Assay, Promega Corporation), which monitors the number of viable cells after 4 hours in medium containing MTS. The conversion of MTS to formazan was measured in a plate reader at 490 nm. The colony formation assay was used to reflect anchorage-independent cell growth. About 1×10^4 cells were layered in 60-mm plate, the medium was replenished every 5 days, and colonies that grew beyond 50 μm in diameter after 3 weeks were scored as countable. Recombinant *SPARCL1* protein (AF2728, R&D) was added into the medium at the concentration of 1 μg/μL. The mean and SD were calculated from 3 independent experiments.

In vitro cell migration and invasion assay

Wound-healing assay was used to measure the ability of cell migration, 2×10^5 viable cells were mixed thoroughly and seeded in 6-well plates. Twenty-four hours after seeding, the cell formed monolayer. A linear wound was created by scraping the cell monolayer with a 200-μL sterile pipette tip. The media were carefully changed to remove any floating cells and cultured at 5% CO_2 and 37 °C for another 24 hours. To elucidate the role of *SPARCL1* protein in wound healing, recombinant *SPARCL1* protein was added into the medium at a concentration of 500 ng/μL. Cells that spread into the scraped region were considered migrating cells. The ability of migration was represented by the migrating distance. To further validate the wound-healing assay, Boyden chamber (BD) was used with interleukin (IL)-8 as a chemoattractant at the concentration of 1 μg/μL. A Matrigel chamber (BD) was used to evaluate the invasion ability of cancer cells. Assays were conducted in 24-well plates with an 8-μm polycarbonate filter membrane coated with growth factor–reduced Matrigel diluted in 20%. Cells in serum-free medium (2.5×10^4 cells per well) were added to the upper chambers. Conditioned medium with 10% FBS was placed in the lower chambers as a chemoattractant. The chambers were incubated for 24 hours at 37°C with 5% CO_2. Migrated cells on the undersides of filter membrane were fixed in 90% (v/v) ethanol and stained with crystal violet. The migrated cells were counted using light microscopy and the experiments were carried out in triplicate.

Construction of xenograft mouse models

All animal experiments were carried out under an approved protocol from the Institutional Animal Care and Use Committee (IACUC) of City of Hope (COH; Duarte, CA). For subcutaneous xenograft mouse model, fifteen 6-week-old male athymic nude mice (BALB/$c^{nu/nu}$) were divided into 3 groups: RKO (group 1), RKO-pLXSN (group 2), and RKO-*SPARCL1* (group 3). Five mice of each group were injected subcutaneously with 5×10^6 viable tumor cells at the site of costal region. Tumor size was measured every 3 days. Tumor volume was calculated on the basis of length and width (20) and plotted against days postinjection. The mice were euthanized on day 23 postinjection or when tumor diameter became larger than 1,000 mm^3. The fresh tumor specimen was divided into 2 parts. One part was fixed with 10% formalin and embedded in paraffin for histologic examination; another part was snap-frozen and stored at −80°C for mRNA and protein extraction.

For liver metastasis mouse model, 6-week-old male athymic nude mice (BALB/$c^{nu/nu}$) were grouped as mentioned above. Under sterilization, mice were anesthetized with pentobarbital sodium. A transverse incision was made in the left flank to expose the spleen. Total of 5×10^6 viable tumor cells were injected into the spleen vein carefully to avoid extravasations. After 5 minutes postinjection, the spleen was excised via ligation at the hilum of the spleen. The mice were euthanized at the day 40 postoperation. Abdominal autopsy was conducted to examine liver metastatic nodules. Histologic examination was further committed by pathologists.

Design of outcome study

This is a retrospective population-based outcome study. The design of study is described in Supplementary Fig. S2. The protocol of human subject application was reviewed and approved by the Institutional Review Board (IRB) of City of Hope and Second Affiliated Hospital of Zhejiang University (ZJU; Hangzhou, Zhejiang, China), respectively. All eligible participants received surgical operation and were diagnosed as colon or rectal adenocarcinoma. A total of 222 CRCs during 1980 to 2004 from COH (training set) and 412 CRCs during 1999 to 2006 from ZJU (validation set) were collected separately according to the following inclusion criteria: (i) diagnosis of CRC by pathologist; (ii) informed consent obtained; and (iii) follow-up data available. The exclusion criteria included: (i) no histologic diagnosis; (ii) informed consent unobtainable; (iii) no follow-up data available; and (iv) multiple cancers. The participants in the COH set included 185 Caucasian, 5 African-American, 13 Asian, and 19 unknown ethnicity. All patients were Asian (Chinese) in the ZJU set. After surgical treatment, all patients were followed up until June 2007 for COH set and September 2010 for ZJU set. The median follow-up period is 166 months in COH set and 46 months in ZJU set. All demographic data and pathologic information were obtained by reviewing the hospital records (Supplementary Table S2). Follow-up data of COH set were obtained from cancer registry at COH. For ZJU set, it was obtained from a

Downloaded from http://aacrjournals.org/clincancerres/article-pdf/18/19/5438/2005391/5438.pdf by guest on 23 May 2025

follow-up work team. Variables assessed included age, gender, date of operation, tumor location (colon or rectal), differentiation, tumor node metastasis (TNM) stage, adjuvant chemotherapy, radiotherapy, date of last follow-up, and vital status at last follow-up. In ZJU, 88 patients were treated with chemotherapy and 3 with radiotherapy. For 222 cases in COH, 90 patients obtained postsurgery chemotherapy and 44 cases received radiotherapy. The chemotherapy regimen in both center is based on 5-fluorouracil. The survival period was calculated from the date of surgical operation to the date patient was last seen. Only deaths from metastasis and local relapse of CRCs were considered as disease-related death.

IHC staining

Formalin-fixed, paraffin-embedded (FFPE) cancer tissues from surgery were selected to construct multiple tissue board (MTB) for COH set and multiple tissue array (MTA) for ZJU set (21). The condition of IHC staining for *SPARCL1* was optimized on checkerboards with different normal and tumor samples. For each IHC staining, negative and positive checkerboards were included for quality control. Standard indirect immunoperoxidase procedures were used for immunohistochemistry. Briefly, 4-μm thick sections were cut from paraffin-embedded tissue blocks, and immunostaining for each antigen was conducted using the avidin–biotin–peroxidase complex technique (MaxVision HRP-Polymer IHC Kit, MAIXIN. Bio), following the manufacturer's instructions. Anti-human *SPARCL1* monoclonal antibody (No.C11; 1:50 dilution) was used as the primary antibody. The slides resulting from the IHC reaction were evaluated individually and independently by 2 investigators in a double-blinded manner. According to the percentages of positive cells and staining intensity, the IHC result was assessed. Despite the heterogeneity of cancer cells, only cytoplasmic signal of *SPARCL1* was considered.

Data management and statistical consideration

MS-ACCESS was used to create a colorectal database. Double entries and logic correction were applied to reduce mistakes in the database. The JMP Statistical Discovery Software (SAS Institute) was used for data analysis. The sample size estimation was calculated using nQuery Advisor 6.01 software. It was indicated that 200 cases would be sufficient for 80% study power with a 2-sided α of 0.05. Multivariate logistic regression models were used to adjust for covariate effects on the ORs. Kaplan–Meier survival analysis and Cox hazard proportional model were used for evaluation of overall survival (OS). ANOVA was used for multiple comparisons. A P value less than 0.05 was considered as statistically significant.

Results

SPARCL1 suppresses proliferation, migration, and invasion of colon cancer cells

The mRNA level of *SPARCL1* was barely detectable in most of colorectal tumor cell lines including RKO and SW620 (Supplementary Fig. S3A). To investigate the role on malignancy, the *SPARCL1* expression plasmid (pLXSN-*SPARCL1*) and control vector (pLXSN) were transfected into RKO and SW620 cells. Stably expressing transfectants (RKO-*SPARCL1*, SW620-*SPARCL1*, as well as the corresponding vector controls) were isolated. Western blot analyses confirmed that the protein level of *SPARCL1* was significantly higher in the expression transfectants than in vector controls after normalizing to β-actin (Fig. 1A, top). The secretion of *SPARCL1* protein was also elevated in the culture medium of *SPARCL1*-transfected cells (Fig. 1A, bottom). In the cell proliferation study conducted using cell counting method, the growth of *SPARCL1* transfectants decreased significantly both in RKO (day 6, $P = 0.03$) and SW620 (day 6, $P = 0.04$) cells in comparison with corresponding vector control (Supplementary Fig. S3B, top). In addition, when the MTS method was used to assess cell proliferation, it showed that the growth of *SPARCL1* transfectants decreased both in RKO (day 5, $P > 0.05$) and SW620 (day 5, $P > 0.05$) cells compared with the vector control (Supplementary Fig. S3B, bottom). The ability of anchorage-independent growth also reflects the potential of cancer metastasis. Consistently, the colony formation of RKO-*SPARCL1* and SW620-*SPARCL1* was dropped by 54% to 62% ($P < 0.01$) and 19% to 48% ($P = 0.03$), respectively, which indicated that anchorage-dependent growth was retarded in *SPARCL1*-expressing cells (Fig. 1B). Recombinant *SPARCL1* peptide significantly reduced the colony formation by RKO cells ($P < 0.01$), as well as SW620 cells ($P < 0.01$; Supplementary Fig. S3C).

The abilities to migrate and invade were regarded as the main malignant phenotype and prerequisite of metastasis for cancer cells. In wound-healing assay, it was shown that the *SPARCL1* transfectants significantly reduced the migration ability of RKO cells (Fig. 1C, $P = 0.03$), as well as SW620 cells ($P = 0.03$). Recombinant *SPARCL1* protein also inhibits cell migration (Supplementary Fig. S3D, $P = 0.03$ in RKO cells and $P > 0.05$ in SW620 cells). The Matrigel invasion assay showed that the invasion ability of *SPARCL1* transfectants decreased significantly (Fig. 1D, $P = 0.01$). The invasion ability was significantly enhanced when we applied IL-8 as chemoattractant in both RKO and SW620 cells ($P < 0.01$), whereas it was significantly reduced by the recombinant *SPARCL1* peptide ($P < 0.01$; Supplementary Fig. S3E).

Above findings suggested that *SPARCL1* could significantly reduce abilities of cell proliferation, anchorage-independent growth, and invasion in colon cancer cell lines.

SPARCL1 inhibits tumor growth and liver metastasis in a mouse xenograft model

To validate the above findings, mouse xenograft models were used to determine whether *SPARCL1* impacts tumor growth and metastasis *in vivo*. The RKO, RKO-pLXSN, or RKO-*SPARCL1* cells were implanted subcutaneously to form xenograft tumors. The tumor volume was monitored every 3 days. The average tumor volume of RKO-*SPARCL1* group was significantly reduced when compared with RKO

Downloaded from http://aacrjournals.org/clincancerres/article-pdf/18/19/5438/2005391/5438.pdf by guest on 23 May 2025

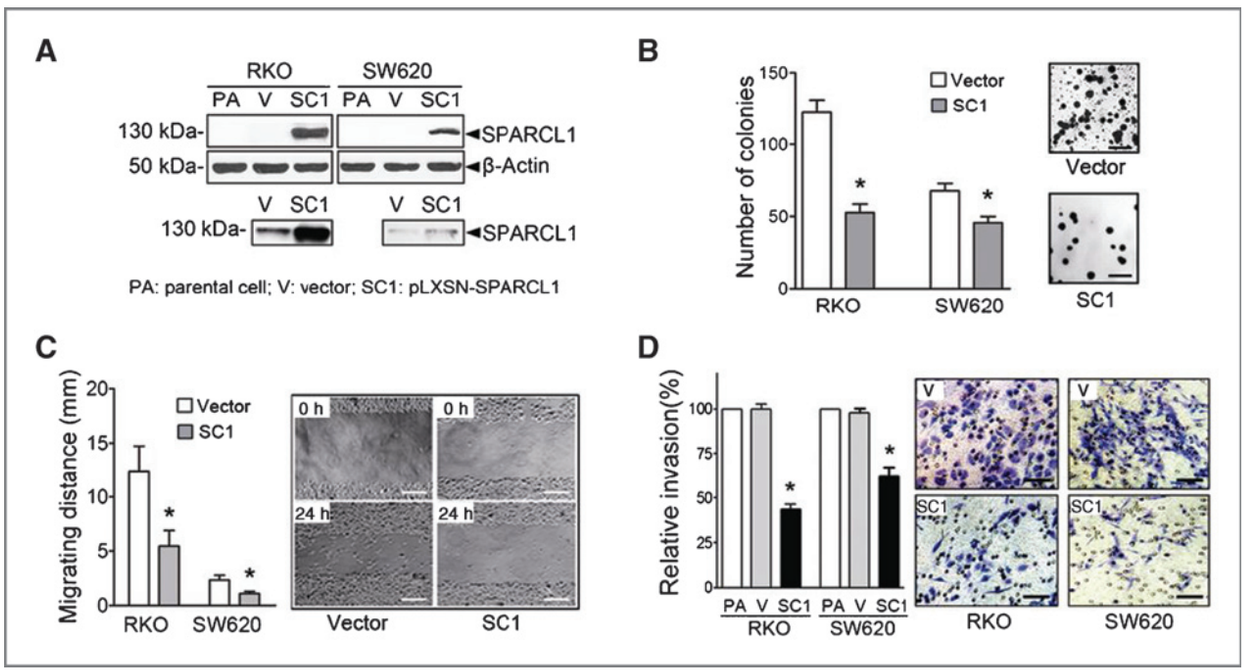

Figure 1. *SPARCL1* reversed malignant phenotypes and induced differentiation of colon cancer cells *in vitro*. A, two *SPARCL1* expression clones (RKO-*SPARCL1* and SW620-*SPARCL1*) were created by transfecting with *SPARCL1* expression plasmid pLXSN-*SPARCL1*, and vector control was constructed using pLXSN. The protein expression of *SPARCL1* was determined by RT-PCR and Western blotting with β-actin as a loading control. *SPARCL1* protein in cell culture medium was also detected by Western blotting. B, anchorage-independent growth reduced in *SPARCL1* expression cell line (SC1) compared with vector control (V) cells (*, $P = 0.03$). Figures are shown on right (scale bar, 100 μm). C, wound-healing assay showed that *SPARCL1* expression inhibited migration of RKO and SW620 cells after treatment for 24 hours (*, $P = 0.03$). Representative result of RKO cell migration at 0 and 24 hours are on the right (scale bar, 50 μm). D, relative invasion capacity of *SPARCL1*-expressing cells (SC1) decreased compared with parental cell (PA) and vector control (V) in RKO and SW620 (*, $P < 0.01$). The representative images of invasive cells are shown on right (scale bar, 50 μm).

group or RKO-pLXSN group (Supplementary Fig. S4). Through RT-PCR, the presence of human *SPARCL1* in RKO-*SPARCL1* xenografts was verified but it was undetectable in RKO-pLXSN cells (Supplementary Fig. S4B). Representative gross views showed size disparity between RKO-pLXSN and RKO-*SPARCL1* in subcutaneous xenograft mouse model (Supplementary Fig. S4C, left). The corresponding images for the hematoxylin and eosin (H&E) staining are also shown (Supplementary Fig. S4C, right). IHC staining confirmed that the *SPARCL1* protein was expressed in the RKO-*SPARCL1* xenograft group but absent in the RKO-pLXSN xenograft group (Supplementary Fig. S4D).

Because liver accounts for most of the CRC metastases, the impact of *SPARCL1* on liver metastasis was assessed through intrasplenic implantation, a liver metastasis model described in Materials and Methods. Laparotomy was conducted on all the mice at 40 days after the implantation of tumor cells. It revealed that RKO-pLXSN cells formed on an average 98 metastatic nodules per liver in 5 mice analyzed as detected by dissection microscopy. In contrast, mice implanted with RKO-*SPARCL1* cells formed on an average 11 nodules (Fig. 2A). It indicated that the metastatic nodules formation was significantly suppressed in *SPARCL1*-expressing transfectants ($P < 0.01$). The presence of human *SPARCL1* in each implant tissue sample was determined by RT-PCR (Fig. 2B). Histologic analyses confirmed that the number of micrometastatic lesions was markedly reduced in the livers of mice injected with *SPARCL1*-expressing cells (Fig. 2C). These results indicated that the expression of *SPARCL1* potentially inhibits liver metastasis of RKO cells in an orthotopic mouse model.

The *SPARCL1* expression negatively associates with poor differentiation, lymph node involvement, and distant organ metastasis in CRCs

To address whether *SPARCL1* suppresses the invasiveness of cancers, the optimized immunohistochemistry was applied to determine whether the expression level of *SPARCL1* was associated with the clinical features of CRCs. All patients were enrolled at City of Hope (COH set, 222 cases) and Zhejiang University (ZJU set, 412 cases). The efficacy and specificity of *SPARCL1* antibody was confirmed as described in Materials and Methods. On the basis of the expression level of *SPARCL1* protein, all participants were divided into 4 subgroups: 0 (negative expression), 1 (weak positive), 2 (positive), and 3 (strong positive; Supplementary Fig. S5). Alternately, 0 and 1 were redefined as *SPARCL1*-low, whereas 2 and 3 were attributed to "*SPARCL1*-high." In COH set, 65 of 222 CRC tissue samples were defined as *SPARCL1*-high expression; and in ZJU set, 182 of 412 patients were regarded as *SPARCL1*-high.

Through IHC staining, higher expression of *SPARCL1* was detected in well-differentiated cancers (Supplementary Fig.

Downloaded from http://aacrjournals.org/clincancerres/article-pdf/18/19/5438/2005391/5438.pdf by guest on 23 May 2025

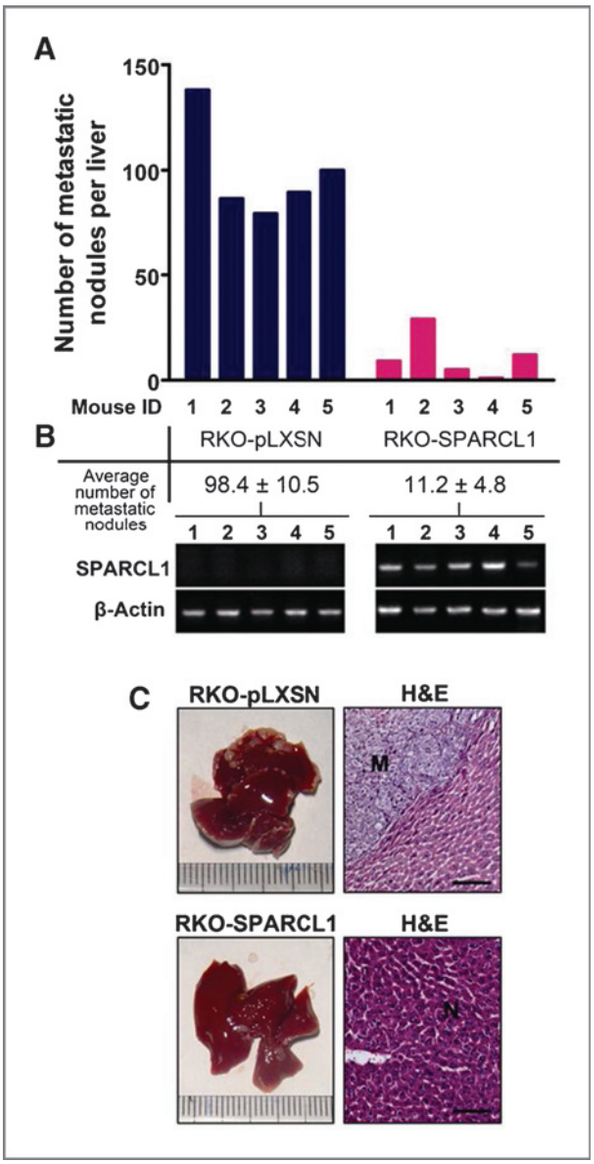

Figure 2. Expression of *SPARCL1* in RKO cells inhibited liver metastasis in xenograft mouse models. A, about 10^6 RKO-pLXSN or RKO-*SPARCL1* cells were injected intrasplenic in BALB/$c^{nu/nu}$ nude mice through microsurgery. After operation, all mice were euthanized for examination on day 40. The number of liver metastatic nodules was reduced in *SPARCL1* transfectants ($P < 0.01$). B, expression levels of human *SPARCL1* in liver metastatic nodules were detected by RT-PCR. C, representative photos of the livers (scale bar, 1 mm), H&E staining of *SPARCL1* of metastatic tumor (M) and normal (N) liver tissues are shown (scale bar, 50 μm).

S5). Statistical analysis revealed that the percentage of *SPARCL1*-high increased with differentiation of CRCs in COH set ($P = 0.06$) and with statistical significance in ZJU set ($P < 0.01$; Table 1). The statistical relevance between *SPARCL1* and metastasis could not be determined in COH set ($P > 0.05$), whereas a high level of *SPARCL1* was negatively associated with lymph node involvement ($P = 0.049$) and distant organ metastasis ($P = 0.01$) in ZJU set (Table 1). Further multivariate logistic analysis revealed that high level of *SPARCL1* expression was negatively related with lymph node involvement [OR, 0.67; 95% confidence interval (CI), 0.45–1.00] and distant metastasis (OR, 0.38; 95% CI, 0.18–0.79) in ZJU set (Table 2).

Above findings suggested that the *SPARCL1* expression correlated with greater differentiation and negatively associated with lymph node involvement and distant metastasis, which implies that *SPARCL1* may function as a tumor suppressor in CRCs.

Higher *SPARCL1* expression is related to better prognosis in CRCs

A retrospective outcome study was conducted on COH set (with 222 CRCs) as well as ZJU set (with 412 CRCs). In Kaplan–Meier analysis, higher expression of *SPARCL1* was associated with better survival in COH set (Fig. 3A, log-rank: $P = 0.05$, univariate COX analysis: $P = 0.045$). In ZJU set, OS was improved significantly in patients with CRCs with higher *SPARCL1* expression (Fig. 3B, log-rank: $P < 0.01$). Multivariate Cox analysis was conducted to eliminate the confounder effects and further validate whether *SPARCL1* was associated with lower relative risk of death from CRCs. The multivariate Cox proportional hazard analysis showed that high expression of *SPARCL1* represented the better survival of CRC (HR, 0.33; 95% CI, 0.33–1.05) in COH set (Fig. 3C); this finding was also confirmed in ZJU set (HR, 0.57; 95% CI, 0.39–0.84; Fig. 3D). The pattern of HRs of other cofactors including metastasis, lymph node involvement, tumor invasion, differentiation, tumor location, gender, and age are very similar, confirming the reliability of this study. To exclude the effect of chemotherapy, a multivariate Cox analysis was conducted on patients without adjuvant chemotherapy or radiotherapy. It indicated that after adjusting for age, gender, location, differentiation, and TNM stage, HR of OS is 0.47 (95% CI, 0.19–1.06) for COH set and 0.61 (95% CI, 0.38–0.98) for ZJU set. These findings suggest that higher *SPARCL1* expression in primary tumor leads to better survivability of patients with CRCs.

The stratification analysis was further used to eliminate the confounders and explore whether *SPARCL1* impacts prognosis differently in patients with CRCs with different TNM stages or tumor locations. For the colon cancer subgroup, the multivariate Cox analyses revealed that *SPARCL1* was related to better OS (HR, 0.63; 95% CI, 0.33–1.13) in COH set (Supplementary Fig. S6A, left). The similar result could be seen in ZJU set (HR, 0.53; 95% CI, 0.31–0.89; Supplementary Fig. S6A right). However, *SPARCL1* seems not to impact the OS of patients with rectal cancer in either COH set or ZJU set (Supplementary Table S3).

Further analysis of CRCs at different TNM stages indicated that *SPARCL1* predicts better survival for both stage I–II CRCs (without metastasis) and stage III–IV CRCs (with metastasis). For stage I–II CRCs, Kaplan–Meier analysis indicated that *SPARCL1* is associated with better survival in COH set (log-rank: $P = 0.06$; Supplementary Fig. S6B, left). It was consistent with results yielded from ZJU set (log-rank: $P = 0.023$; Supplementary Fig. S6B, right).

Downloaded from http://aacrjournals.org/clincancerres/article-pdf/18/19/5438/2005391/5438.pdf by guest on 23 May 2025

Table 1. Pathoclinical characteristics and *SPARCL1* distribution of eligible CRCs from COH and ZJU

	COH set ($N = 222$)			ZJU set ($N = 412$)		
	No. of cases	No. of *SPARCL1*-high[a] (%)	*P*	No. of cases	No. of *SPARCL1*-high[a] (%)	*P*
Age[b], y						
<40	9	2 (22.2)		37	19 (51.4)	
40–49	17	3 (17.7)		64	23 (35.9)	
50–59	50	10 (20.0)		106	50 (47.2)	
60–69	65	19 (29.2)		92	40 (43.5)	
70–79	61	23 (37.7)		90	39 (43.3)	
≥80	20	8 (40.0)	0.252	21	11 (52.4)	0.62
Gender						
Male	113	37 (32.7)		252	106 (42.1)	
Female	109	28 (25.7)	0.248	160	76 (47.5)	0.279
Location						
Colon	169	55 (32.5)		222	97 (43.7)	
Proximal[c]	99	32 (32.3)		110	46 (41.8)	
Distal[d]	70	23 (32.9)		112	51 (45.5)	
Rectum	53	10 (18.9)	0.161	190	85 (44.7)	0.387
Differentiation[e]						
Poorly	19	3 (15.8)		82	25 (30.5)	
Moderately	174	54 (31.0)		171	71 (41.5)	
Well	19	6 (31.6)	0.06	159	86 (54.1)	0.001[g]
Tumor invasion[f]						
T0–T2	23	6 (26.1)		77	36 (46.8)	
T3 and T4	191	58 (30.4)	0.672	332	145 (43.7)	0.624
Lymph node involvement						
Negative	167	46 (27.5)		229	111 (48.5)	
Positive	55	19 (34.6)	0.322	183	71 (38.8)	0.049[g]
Distant metastasis						
No	180	53 (29.4)		372	172 (46.2)	
Yes	42	12 (28.6)	0.911	40	10 (25.0)	0.010[g]

[a]*SPARCL1*-high includes positive and strong positive of cytoplasm staining score.

[b]In ZJU set, there are 2 cases without data.

[c]Proximal colon includes cecum, appendix, ascending colon, hepatic flexure, transverse, and splenic flexure.

[d]Distal colon includes descending colon and sigmoid.

[e]In COH set, there are 10 cases without differentiation data.

[f]According to the NCCN Clinical Practice Guidelines in Oncology Colon Cancer (V.3.2011) and Rectal Cancer (V.I.2011). In COH set, there are 8 cases without tumor invasion data; and in ZJU set, there are 3 cases without data.

[g]Statistical significance, $P < 0.05$.

Meanwhile, *SPARCL1* predicting better survival was also seen in patients with CRCs with stage III–IV (Supplementary Fig. S6C). Multivariate analysis also displayed similar results (Supplementary Table S3). It was indicated the *SPARCL1* independently prognoses better survival of CRCs with early or later stages.

The above findings showed that *SPARCL1* may serve as a potential prognostic biomarker and prognosticate better survival for patients with CRCs, especially for colon cancers.

SPARCL1 relates to the differentiation of CRCs via mesenchymal–epithelial transition

To explore the mechanism of *SPARCL1* in malignancy suppression, the *SPARCL1* and differentiation of CRCs were investigated. The IHC staining showed that *SPARCL1* expression in colon cancer section eventually decreased in comparison with adjacent normal colon section (Fig. 4A, i–iii). Meanwhile, *SPARCL1* steadily increased with poor, moderate, and well differentiation of CRCs (Fig. 4A, iv–vi). The lumen-like formation indicated the ability to differentiate. An *in vitro* study showed that upregulation of *SPARCL1* by gene transfection could obviously enhance the lumen-like formation in Matrigel in RKO and SW620 cells (Fig. 4B). Correspondingly, recombinant *SPARCL1* peptide also could promote the lumen-like formation (Fig. 4B). The *E-cadherin*, *N-cadherin*, and *Vimentin* were regarded as the mesenchymal–epithelial transition (MET)-related genes. It was indicated that the mRNA expression level of *E-cadherin*

Downloaded from http://aacrjournals.org/clincancerres/article-pdf/18/19/5438/2005391/5438.pdf by guest on 23 May 2025

Table 2. Logistic analysis for *SPARCL1* and TNM stages of CRCs

	COH set ($N = 222$)			ZJU set ($N = 412$)		
	No. of cases	OR (95% CI)	Adjusted OR[a] (95% CI)	No. of cases	OR (95% CI)	Adjusted OR[a] (95% CI)
Tumor invasion[b]						
T0–T2	23	Reference	Reference	77	Reference	Reference
T3 and T4	191	0.81 (0.28–2.06)	0.76 (0.26–1.98)	332	0.89 (0.58–1.35)	0.89 (0.58–1.35)
Lymph node involvement						
Negative	167	Reference	Reference	229	Reference	Reference
Positive	55	0.72 (0.38–1.40)	0.67 (0.34–1.31)	183	0.67[c] (0.45–1.00)	0.66 [c] (0.45–0.99)
Distant metastasis						
No	180	Reference	Reference	372	Reference	Reference
Yes	42	1.04 (0.51–2.26)	0.89 (0.42–1.96)	40	0.38 [c] (0.18-.0.79)	0.38 [c] (0.17–0.79)

NOTE: Logistic analysis was conducted to evaluate OR of *SPARCL1* (high vs. low).

[a]Adjusted by gender and age.

[b]According to the NCCN Clinical Practice Guidelines in Oncology Colon Cancer (V.3.2011) and Rectal Cancer (V.3.2011). In COH set, there are 8 cases without tumor invasion data; and in ZJU set, there are 3 cases without data.

[c]Statistical significance, $P < 0.05$.

was significantly upregulated on RKO-*SPARCL1* and SW620-*SPARCL1* transfectants, and *N-cadherin* and *Vimentin* were significantly downregulated (Fig. 4C). The Western blot analysis further confirmed that increase of *E-cadherin* and decrease of *N-cadherin* and *Vimentin* could be seen in *SPARCL1*-expressing RKO and SW620 transfectants (Fig. 4D). Meanwhile, qRT-PCR analysis also showed that the differentiation-related genes *GPNMB, NDRG1, and IGF1R* were significantly upregulated on RKO-*SPARCL1* transfectants (Supplementary Fig. S3F). Above findings suggest that *SPARCL1* induces differentiation through MET in colon cancer cells.

Discussion

In this study, we showed that *SPARCL1* suppresses the proliferation, migration, invasion, and anchorage-independent growth of colon cancer cells (Fig. 1). The expression of *SPARCL1* also induces the differentiation of colon cancer cells (Fig. 4). The results are consistent with previously conducted *in vitro* studies (8, 22). Here, we further report the *in vivo* findings obtained using xenograft animal models. In the subcutaneous xenograft mouse model, the expression of *SPARCL1* retarded tumor growth, which points to its antiproliferation potential (Supplementary Fig. S4). We used an intrasplenic injection mouse model mimicking liver metastasis of CRC at the later stages. This was based on the anatomy assumption that colon cancer cells migrate mostly through vena porta hepatic (23). The liver metastasis animal model indicated that *SPARCL1* significantly reduces the liver metastasis by RKO cells (Fig. 2). These *in vitro* and *in vivo* studies validate that the expression of *SPARCL1* has potential malignancy-suppressing ability in colon cancer cells.

In the outcome study, expression of *SPARCL1* was significantly related to better survival of CRCs in 2 sets of patients with different socioeconomic backgrounds. The *SPARCL1* expression was associated with well differentiation in patients from COH set ($P = 0.06$) and ZJU set ($P < 0.01$), which was consistent with the *in vitro* studies. *SPARCL1* reduced the relative risk of lymph node involvement (OR, 0.66; 95% CI, 0.45–0.99) and distant organ metastasis (OR, 0.38; 95% CI, 0.17–0.79) in ZJU set. Besides the CRCs, downregulation of *SPARCL1* was also reported for prostate and pancreatic cancers (22). Kaplan–Meier and Cox proportional hazard analyses revealed that *SPARCL1* functions as a protective factor. It prognosticates better survival of patients with CRCs both in COH set (HR, 0.33; 95% CI, 0.33–1.05) and ZJU set (HR, 0.57; 95% CI, 0.38–0.84). The protective effect of *SPARCL1* could be observed in the ZJU set (Fig. 3B, Supplementary Fig. S6B and S6C, right). Whether *SPARCL1* plays protective role in rectal cancers awaits further confirmation. A Swedish research team reported that *SPARCL1* was positively associated with well differentiation, which is consistent with our findings (19). However, their patient-based data indicated that *SPARCL1* prognosticates poor survival in CRCs (19). The opposing results by 2 research teams may be due to different antibodies that were used for immunohistochemistry. We tested the commercial antibody (R&D) and found many nonspecific signals on Western blot analysis (Supplementary Fig. S1). Therefore, we developed a new antibody (No.C11) and showed that the nonspecific signals of No.C11 were barely seen on Western blot analysis (Supplementary Fig. S1). Meanwhile, the intensity of specific signal detected by our antibody correlates with the *SPARCL1* mRNA level (Fig. 1A). The signal was blocked by *SPARCL1* peptide (Supplementary Fig. S1), indicating the reliability of our IHC staining technique.

The above evidence showed the malignancy-suppressing ability of *SPARCL1*. Nevertheless, its function still remains largely unknown. In the previous studies, *SPARCL1* was

Downloaded from http://aacrjournals.org/clincancerres/article-pdf/18/19/5438/2005391/5438.pdf by guest on 23 May 2025

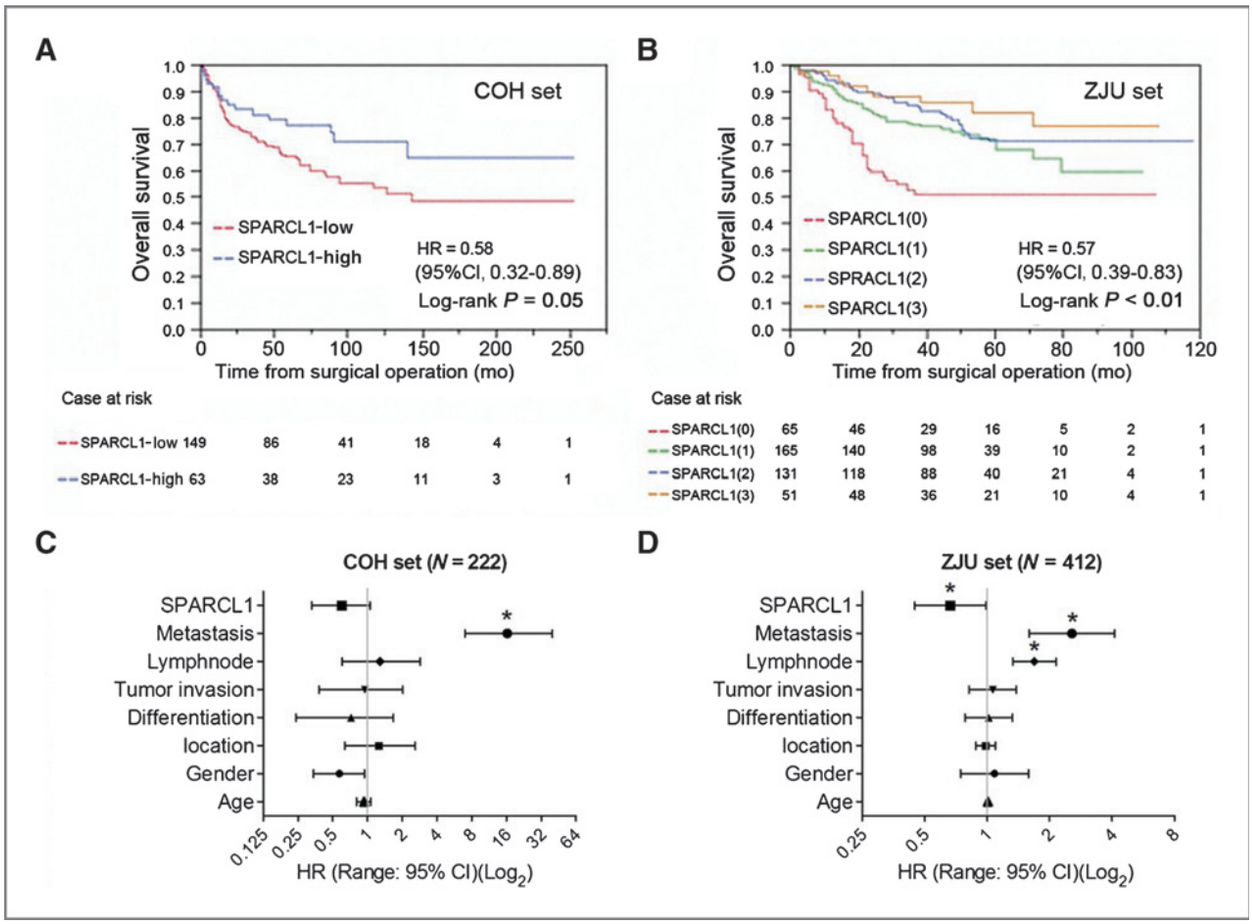

Figure 3. Higher expression level of *SPARCL1* is related to better prognosis of CRCs. The *SPARCL1* protein expression levels were scored on the basis of density of IHC staining. The score 0 is negative staining, 1 is weak positive, 2 is positive, and 3 is strong positive (Supplementary Fig. S5). To fit the Cox analysis, the expression of *SPARCL1* was recategorized as *SPARCL1*-low (scores 0 and 1) and *SPARCL1*-high (scores 2 and 3). A, Kaplan–Meier analysis for OS was displayed as *SPARCL1*-high versus *SPARCL1*-low to enhance the study power in COH set. B, Kaplan-Meier analysis for OS was conducted in ZJU set. The multivariate Cox analyses for OS of CRCs are shown in C and D for COH set and ZJU sets, respectively. The HR of *SPARCL1* was based on *SPARCL1*-high versus *SPARCL1*-low; tumor invasion was T3–T4 versus T0–T2; lymph node was positive versus negative; metastasis was yes versus no; differentiation was histologic grade II and III versus grade I; tumor location was rectum versus colon; gender was female versus male; age was based on per unit changes. *, statistical significance ($P < 0.05$).

regarded as an astrocyte marker (24) and was proved to be essential in regulating cell–matrix interaction in the development of the brain (25). Increase in *SPARCL1* was reported during the differentiation of embryonic stem cells into astrocytes (26). Our *in vitro* experiment showed that *SPARCL1* induced the ability of luminal-like structure formation in Matrigel (Fig. 4B). It implied that the induction of differentiation could partly explain the malignancy suppression by *SPACRL1*. The correlation and differentiation of *SPARCL1* was also confirmed in a population-based study (Table 1).

SPARCL1 may function as a tumor suppressor by inducing differentiation. Our data indicated that *SPARCL1* expression was increased with well differentiation in CRCs. Colon cancer cells transfected with *SPARCL1* or cultured with *SPARCL1* peptide showed morphology diversity from the parental cell lines, which exhibited a luminal-like growth pattern. The *E-cadherin* was considered as epithelial marker; the *N-cadherin* and *Vimentin* were mesenchymal markers in epithelial–mesenchymal transition (EMT; refs. 27, 28). Our findings also suggested that that *SPARCL1* induced differentiation probably by MET. Both qRT-PCR and Western blot analysis showed increase of *E-cadherin* and decrease of *N-cadherin* and *Vimentin* in RKO-*SPARCL1* and SW620-*SPARCL1* transfectants (Fig. 4C and D). On other hands, previous studies showed that *GPNMB*, *NDRG1*, and *IGF1R* were cell differentiation markers (29–31). *GPNMB* (Glycoprotein NMB, Osteoactivin) was reported to be an essential protein during the differentiation of osteoblast (32). N-Myc downstream–regulated gene 1 (*NDRG1*), also named differentiation-related gene-1, is involved in the development of central nervous system (33). *NDRG1* was reported as a differentiation marker of breast cancer (34) and prognosticates better survival in CRCs (35). The *IFG1R* was considered as another differentiation-related gene in lung adenocarcinoma (29). Here, the results indicated that

Downloaded from http://aacrjournals.org/clincancerres/article-pdf/18/19/5438/2005391/5438.pdf by guest on 23 May 2025

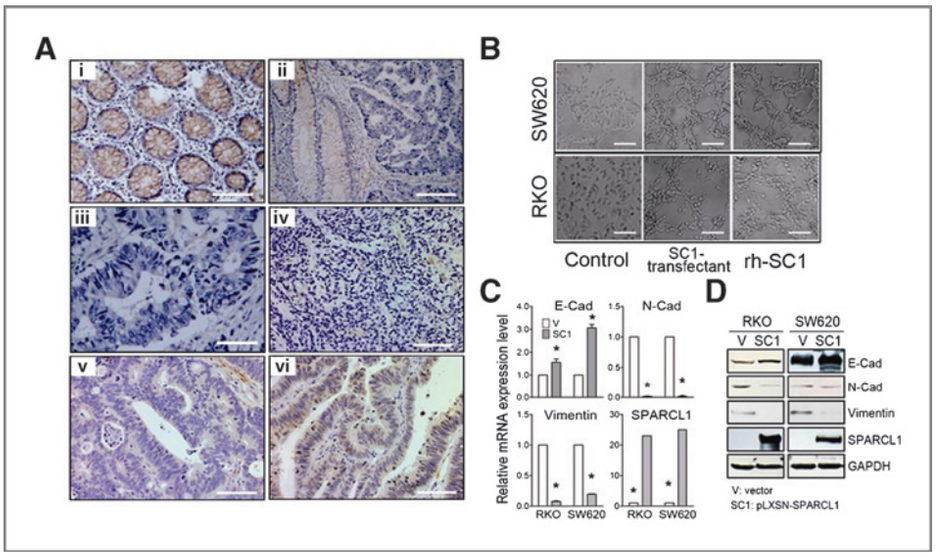

Figure 4. *SPARCL1* was related to differentiation of CRC via inducing MET. A, IHC staining of *SPARCL1* showed in adjacent normal colon epithelium (i), connection between normal and cancerous sections (ii), and colon cancer section (iii). The *SPARCL1* expression increases with grade with poor (iv), moderate (v), and well (vi) differentiation, respectively. The scale bar represents 50 μm in (i), (iv), (v), and (vi); 100 μm in (ii); and 20 μm in (iii). B, colon cell formed luminal-like formation after transfection with *SPARCL1* or treated with recombinant *SPARCL1* protein (1 μg/μL). Scale bar, 50 μm. C, overexpression of *SPARCL1* caused changes of *E-cadherin*, *N-cadherin*, and *Vimentin* in mRNA levels. The qRT-PCR analysis showed downregulation of *N-cadherin* and *Vimentin* and up-regulation of *E-cadherin* in stable *SPARCL1* overexpression transfectants (*, $P < 0.01$). D, Western blot analysis showed the protein level of *N-cadherin*, *Vimentin*, and *E-cadherin*. The glyceralde-3-phosphate dehydrogenase (*GAPDH*) was used as a loading control.

the transcripts of *GPNMB*, *NDRG1*, and *IGF1R* were significantly increased in *SPARCL1* transfectants (Supplementary Fig. S3F). On the basis of these studies, we inferred that loss of *SPARCL1* in colon epithelial might lead to deficiency of differentiation and achievement of carcinogenesis by reducing MET. Therefore, induction of differentiation may, at least, be one of the pathways through which *SPARCL1* suppresses malignancy in CRCs. *SPARCL1* might be a potential differentiation marker for CRCs. Nevertheless, the detail mechanism of *SPARCL1* during MET process needs to be further investigated.

Overall, the above findings revealed that *SPARCL1* is a potential tumor suppressor gene mediating cell differentiation, inhibiting proliferation ability, and reducing cell invasion and metastasis potential. Thus, it relates to better prognosis in patients with CRCs.

Disclosure of Potential Conflicts of Interest

No potential conflicts of interest were disclosed.

Authors' Contributions

Conception and design: H. Hu, H. Zhang, X. Liu, S. Yu, S. Zhang, Y. Yen, S. Zheng

Development of methodology: H. Hu, H. Zhang, X. Liu, S. Loera, J. Peng, S. Yu

Acquisition of data (provided animals, acquired and managed patients, provided facilities, etc.): H. Hu, H. Zhang, W. Ge, S. Loera, P. Chu, H. Chen, J. Peng, L. Zhou, S. Yu, L. Lai

Analysis and interpretation of data (e.g., statistical analysis, biostatistics, computational analysis): H. Hu, H. Zhang, W. Ge, X. Liu, P. Chu, S. Yu, S. Zheng

Writing, review, and/or revision of the manuscript: H. Hu, H. Zhang, X. Liu, L. Lai, Y. Yen, S. Zheng

Administrative, technical, or material support (i.e., reporting or organizing data, constructing databases): H. Hu, H. Zhang, J. Peng, L. Zhou, S. Yu, Y. Yen

Study supervision: H. Hu, Y. Yuan, S. Zhang, L.L. Lai,Y. Yen, S. Zheng

Acknowledgments

The authors thank Lifang Yao for technical assistance with tissue blocks and slide preparation and Mariko Lee from the Microscope Core Lab, City of Hope, for technical assistance with acquisition of IHC microscopy images. They also thank Mansze Kong and Dr. Frank Hong for helping on English editing.

Grant Support

This work was supported by grants from National High-tech R&D Program of China (863 Program, No. 2012AA02A506), the National Natural Science Foundation of China (No. 81000892 and No. 81101477), Zhejiang Provincial Natural Science Foundation of China (No. R2090353), and State-Sponsored Scholarship Program for Graduate Students, China Scholarship Council. This project was also partially supported by the U.S. NIH grants (R01, CA127541).

The costs of publication of this article were defrayed in part by the payment of page charges. This article must therefore be hereby marked *advertisement* in accordance with 18 U.S.C. Section 1734 solely to indicate this fact.

Received January 16, 2012; revised August 3, 2012; accepted August 3, 2012; published OnlineFirst August 13, 2012.

References

1. Siegel R, Ward E, Brawley O, Jemal A. Cancer statistics, 2011: the impact of eliminating socioeconomic and racial disparities on premature cancer deaths. CA Cancer J Clin 2011;61:212–36.

2. Rim SH, Seeff L, Ahmed F, King JB, Coughlin SS. Colorectal cancer incidence in the United States, 1999–2004: an updated analysis of data from the National Program of Cancer Registries and the

Downloaded from http://aacrjournals.org/clincancerres/article-pdf/18/19/5438/2005391/5438.pdf by guest on 23 May 2025

Surveillance, Epidemiology, and End Results Program. Cancer 2009;115:1967–76.
3. Hawk ET, Limburg PJ, Viner JL. Epidemiology and prevention of colorectal cancer. Surg Clin North Am 2002;82:905–41.
4. Jaeck D, Bachellier P, Guiguet M, Boudjema K, Vaillant JC, Balladur P, et al. Long-term survival following resection of colorectal hepatic metastases. Association Francaise de Chirurgie. Br J Surg 1997;84: 977–80.
5. Bendik I, Schraml P, Ludwig CU. Characterization of MAST9/Hevin, a SPARC-like protein, that is down-regulated in non-small cell lung cancer. Cancer Res 1998;58:626–9.
6. Girard JP, Springer TA. Cloning from purified high endothelial venule cells of hevin, a close relative of the antiadhesive extracellular matrix protein SPARC. Immunity 1995;2:113–23.
7. Girard JP, Springer TA. Modulation of endothelial cell adhesion by hevin, an acidic protein associated with high endothelial venules. J Biol Chem 1996;271:4511–7.
8. Claeskens A, Ongenae N, Neefs JM, Cheyns P, Kaijen P, Cools M, et al. Hevin is down-regulated in many cancers and is a negative regulator of cell growth and proliferation. Br J Cancer 2000;82:1123–30.
9. Maak S, Jaesert S, Neumann K, Yerle M, von Lengerken G. Isolation of expressed sequence tags of skeletal muscle of neonatal healthy and splay leg piglets and mapping by somatic cell hybrid analysis. Anim Genet 2001;32:303–7.
10. Oritani K, Kincade PW. Lymphopoiesis and matrix glycoprotein SC1/ ECM2. Leuk Lymphoma 1998;32:1–7.
11. Soderling JA, Reed MJ, Corsa A, Sage EH. Cloning and expression of murine SC1, a gene product homologous to SPARC. J Histochem Cytochem 1997;45:823–35.
12. Johnston IG, Paladino T, Gurd JW, Brown IR. Molecular cloning of SC1: a putative brain extracellular matrix glycoprotein showing partial similarity to osteonectin/BM40/SPARC. Neuron 1990;4:165–76.
13. Girard JP, Baekkevold ES, Yamanaka T, Haraldsen G, Brandtzaeg P, Amalric F. Heterogeneity of endothelial cells: the specialized phenotype of human high endothelial venules characterized by suppression subtractive hybridization. Am J Pathol 1999;155: 2043–55.
14. Isler SG, Schenk S, Bendik I, Schraml P, Novotna H, Moch H, et al. Genomic organization and chromosomal mapping of SPARC-like 1, a gene down regulated in cancers. Int J Oncol 2001;18:521–6.
15. Lau CP, Poon RT, Cheung ST, Yu WC, Fan ST. SPARC and Hevin expression correlate with tumour angiogenesis in hepatocellular carcinoma. J Pathol 2006;210:459–68.
16. Nelson PS, Plymate SR, Wang K, True LD, Ware JL, Gan L, et al. Hevin, an antiadhesive extracellular matrix protein, is down-regulated in metastatic prostate adenocarcinoma. Cancer Res 1998;58:232–6.
17. Notterman DA, Alon U, Sierk AJ, Levine AJ. Transcriptional gene expression profiles of colorectal adenoma, adenocarcinoma, and normal tissue examined by oligonucleotide arrays. Cancer Res 2001;61:3124–30.
18. Yu SJ, Yu JK, Ge WT, Hu HG, Yuan Y, Zheng S. *SPARCL1*, Shp2, MSH2, E-cadherin, p53, ADCY-2 and MAPK are prognosis-related in colorectal cancer. World J Gastroenterol 2011;17:2028–36.
19. Zhang H, Widegren E, Wang DW, Sun XF. *SPARCL1*: a potential molecule associated with tumor diagnosis, progression and prognosis of colorectal cancer. Tumour Biol 2011;32:1225–31.
20. Gasparini G, Harris AL. Clinical importance of the determination of tumor angiogenesis in breast carcinoma: much more than a new prognostic tool. J Clin Oncol 1995;13:765–82.
21. Meng PQ, Hou G, Zhou GY, Peng JP, Dong Q, Zheng S. Application of new tissue microarrayer-ZM-1 without recipient paraffin block. J Zhejiang Univ Sci B 2005;6:853–8.
22. Esposito I, Kayed H, Keleg S, Giese T, Sage EH, Schirmacher P, et al. Tumor-suppressor function of SPARC-like protein 1/Hevin in pancreatic cancer. Neoplasia 2007;9:8–17.
23. Primrose JN. Surgery for colorectal liver metastases. Br J Cancer 2010;102:1313–8.
24. Kucukdereli H, Allen NJ, Lee AT, Feng A, Ozlu MI, Conatser LM, et al. Control of excitatory CNS synaptogenesis by astrocyte-secreted proteins Hevin and SPARC. Proc Natl Acad Sci U S A 2011;108: E440–9.
25. Weaver MS, Workman G, Cardo-Vila M, Arap W, Pasqualini R, Sage EH. Processing of the matricellular protein hevin in mouse brain is dependent on ADAMTS4. J Biol Chem 2010;285:5868–77.
26. Weimer JM, Stanco A, Cheng JG, Vargo AC, Voora S, Anton ES. A BAC transgenic mouse model to analyze the function of astroglial *SPARCL1* (SC1) in the central nervous system. Glia 2008;56:935–41.
27. Thiery JP. Epithelial-mesenchymal transitions in development and pathologies. Curr Opin Cell Biol 2003;15:740–6.
28. Baum B, Settleman J, Quinlan MP. Transitions between epithelial and mesenchymal states in development and disease. Semin Cell Dev Biol 2008;19:294–308.
29. Kikuchi R, Sonobe M, Kobayashi M, Ishikawa M, Kitamura J, Nakayama E, et al. Expression of IGF1R is associated with tumor differentiation and survival in patients with lung adenocarcinoma. Ann Surg Oncol 2012;19 Suppl 3:412—20.
30. Lachat P, Shaw P, Gebhard S, van Belzen N, Chaubert P, Bosman FT. Expression of NDRG1, a differentiation-related gene, in human tissues. Histochem Cell Biol 2002;118:399–408.
31. Abdelmagid SM, Barbe MF, Rico MC, Salihoglu S, Arango-Hisijara I, Selim AH, et al. Osteoactivin, an anabolic factor that regulates osteoblast differentiation and function. Exp Cell Res 2008;314:2334–51.
32. Arosarena OA, Del Carpio-Cano FE, Dela Cadena RA, Rico MC, Nwodim E, Safadi FF. Comparison of bone morphogenetic protein-2 and osteoactivin for mesenchymal cell differentiation: effects of bolus and continuous administration. J Cell Physiol 2011;226:2943–52.
33. Fotovati A, Abu-Ali S, Sugita Y, Nakamura Y. Expression of N-myc downstream regulated gene 1 (NDRG1) in central neurocytoma. J Clin Neurosci 2011;18:1383–5.
34. Fotovati A, Abu-Ali S, Kage M, Shirouzu K, Yamana H, Kuwano M. N-myc downstream-regulated gene 1 (NDRG1) a differentiation marker of human breast cancer. Pathol Oncol Res 2011;17:525–33.
35. Strzelczyk B, Szulc A, Rzepko R, Kitowska A, Skokowski J, Szutowicz A, et al. Identification of high-risk stage II colorectal tumors by combined analysis of the NDRG1 gene expression and the depth of tumor invasion. Ann Surg Oncol 2009;16:1287–94.

Downloaded from http://aacrjournals.org/clincancerres/article-pdf/18/19/5438/2005391/5438.pdf by guest on 23 May 2025